

Experimental evidence for the transition from two- to three-dimensional behavior of excitons in quantum-well structures

J.-P. Reithmaier,* R. Höger, and H. Riechert

Siemens Research Laboratories, Otto-Hahn-Ring 6, 8000 München 83, Federal Republic of Germany

(Received 30 August 1990)

The transition from two- to three-dimensional behavior of excitonic recombination was investigated by optical-absorption and photoluminescence (PL) spectroscopy. By molecular-beam epitaxy, we have grown pseudomorphic $\text{In}_x\text{Ga}_{1-x}\text{As}/\text{Ga}(\text{Al})\text{As}$ multiple- and single-quantum-well structures with and without Al in the barriers and with an In content between 13% and 22%. The well width was varied from 25 nm to less than 1 nm. From absorption spectra, we have directly determined the exciton binding energy for the first heavy-hole-to-electron transition and unambiguously for the light-hole-to-electron transition in a sample with a well width of 3 nm. The exciton binding energy nearly reaches the bulk values of the barrier material for very small well widths, e.g., 4.2 ± 0.5 meV for a 1-nm well width with a GaAs barrier. The dependence of the PL linewidth on the well width in single-quantum-well structures shows behavior similar to the exciton binding energy. We also reach the narrowest linewidths (0.6 meV) for the thinnest quantum well (0.75 nm) and a maximum (3 meV) at around a 5-nm well width. Samples with Al in the barriers (14%) show similar behavior, but the linewidths increase by about 30% at larger well widths and more than 100% at narrower wells in comparison to samples with a binary barrier material. These experimental results demonstrate very clearly the transition from an exciton with three-dimensional properties of the well material (at larger well widths) to an intermediate state with a maximum two-dimensional character (at around 5 nm) and once again to a three-dimensional behavior of the exciton with the properties of the barrier material (at well widths less than 4–5 nm). All PL peaks show a fine structure, which can be very accurately fitted by only two Gaussian curves. A comparison between absorption and PL spectra shows that an additional higher-energy PL peak, which can be resolved in the spectra of high-quality samples with narrow linewidths, corresponds to the onset of the exciton continuum.

I. INTRODUCTION

In bulk material the exciton binding energies are well known for many material systems from evaluations of different optical spectra, e.g., photoluminescence (PL), photoluminescence excitation (PLE), photoreflectance, and optical-absorption spectroscopy (OAS).¹ Especially in GaAs a value of 4.2 meV was determined for the 1s exciton state.²

Pseudo-two-dimensional behavior of excitonic transitions is predicted for quantum-well structures. The exciton binding energy should reach a maximum value four times as high as the bulk value.³ Because of the leakage of the wave function into the barrier material, a complete confinement, i.e., the two-dimensional limit, cannot be reached. On the contrary, at zero well width the exciton binding energy should be similar to that of the bulk material of the barriers. An analogous behavior is expected for the linewidth of excitonic transitions,⁴ which was already observed by Bertolet and co-workers^{5,6} for heterostructures with binary wells and ternary barriers.

We have used pseudomorphic $\text{In}_x\text{Ga}_{1-x}\text{As}/\text{GaAs}$ quantum-well structures, because they are promising for electronic and optical devices. The disadvantage of this material system, i.e., dislocations due to the lattice mismatch between $\text{In}_x\text{Ga}_{1-x}\text{As}$ and GaAs, can be avoided by using optimal growth parameters and layer

thicknesses lower than the critical thickness,⁷ above which strain relaxation can occur. But there are also some main advantages in comparison to the $\text{GaAs}/\text{Ga}_y\text{Al}_{1-y}\text{As}$ material system. With pseudomorphic $\text{In}_x\text{Ga}_{1-x}\text{As}$ grown on GaAs substrates, we have the opportunity to use either GaAs or $\text{Ga}_y\text{Al}_{1-y}\text{As}$ as a barrier material. Therefore we can study the influence of the barrier material on the optical properties of the well. An experimental advantage is that the substrate is a wide-gap material, so we can do transmission experiments without difficult sample preparation.

We present a systematic investigation of the transition from three-dimensional to pseudo-two-dimensional behavior of the optical properties of excitonic transitions by varying the well width in $\text{In}_x\text{Ga}_{1-x}\text{As}/\text{GaAs}$ quantum-well structures. After a presentation of the experimental details in Sec. II, we will deal with our topic in two parts. Section III A presents the dependence of the excitonic binding energies on the quantum-well width. We will show that theoretical predictions are qualitatively confirmed while quantitatively for small and large well widths we found lower values for the exciton binding energy than calculated by Moore *et al.*⁸ Section III B is devoted to results and discussions on excitonic linewidths. Again we find the highest values for intermediate well widths where two-dimensional features, such as interface quality, are most important. The smaller linewidths for

both thinner and thicker wells correspond to bulklike properties of barrier and well materials, respectively (with bulklike properties of the $\text{In}_x\text{Ga}_{1-x}\text{As}$ well material we mean the fictive three-dimensional limit of the strained material). Data on ternary $\text{Ga}_y\text{Al}_{1-y}\text{As}$ barriers further support this image.

We also present an absorption spectrum of a light-hole-to-electron transition of a multiple-quantum-well (MQW) sample with 3-nm-thick wells, in which, to our knowledge for the first time, the excitonic peak is unambiguously resolved from the continuum edge.

II. EXPERIMENT

A. Growth details

All samples were grown in a VG V80H molecular-beam-epitaxy system with elemental sources. The layers were deposited on semi-insulating (001) GaAs substrates, which were In free mounted on the substrate holder. The typical growth rate was around $1 \mu\text{m}/\text{h}$. The $\text{As}_4/(\text{In,Ga,Al})$ beam equivalent-pressure ratio was higher than 10 (As stabilized growth). We took much effort in control of the growth temperature to avoid significant In desorption. We use a pyrometer with a detection wavelength of less than $0.97 \mu\text{m}$ for measuring the surface temperature of the substrate during growth. For recalibration of the pyrometer reading we use routinely before each run the oxide desorption point of GaAs at 582°C (Ref. 9) monitored by RHEED (reflection high-energy electron diffraction). All quantum-well structures were grown at a substrate temperature of $(520 \pm 10)^\circ\text{C}$, i.e., also the GaAs ($\text{Ga}_y\text{Al}_{1-y}\text{As}$, respectively) barrier layers.

We employed two kinds of quantum-well structures: (i) $\text{In}_x\text{Ga}_{1-x}\text{As}/\text{GaAs}$ multiple quantum wells with 300-nm-GaAs buffer layers and (ii) $\text{In}_x\text{Ga}_{1-x}\text{As}/\text{Ga}(\text{Al})\text{As}$ single-quantum-well (SQW) sequences with different well widths within one sample and a 300-nm-thick GaAs buffer layer including a $\text{Ga}_y\text{Al}_{1-y}\text{As}/\text{GaAs}$ superlattice structure for additional cleaning purposes.

The sample parameters of the first structure (i) are collected in Table I. Two samples (cf. Table II) are grown according to the second structure (ii), one without Al and one with about 14% Al in the barriers (barrier thickness $\approx 80 \text{ nm}$). No interruptions were applied during growth. The well width was varied from 0.75 nm (< 3 monolayers) to 25 nm (≈ 87 monolayers) in 8 and 9 steps, respectively. The In content has the same value as the MQW's with thin quantum wells ($\approx 13.5\%$). Additionally we have used these structures for calibrating the $\text{In}_x\text{Ga}_{1-x}\text{As}$ growth rate by transmission-electron-microscopy (TEM) analysis, also for the thin MQW samples.

B. Photoluminescence and optical-absorption spectroscopy

The samples were investigated by PL and OAS. For both measurements they were mounted in a variable temperature cryostat, which allows measurements between 1.6 and 300 K .

For PL measurements we used a focused Ar^+ laser beam at an emission wavelength of 514 nm . The luminescence light was dispersed by a 1-m monochromator with a spectral resolution of better than 0.1 meV in a wavelength range of 700 to 900 nm . For collecting the PL light, we have used a GaAs detector for wavelengths shorter than 800 nm ($> 1.41 \text{ eV}$) and a cooled S1 photomultiplier or Ge detector for longer wavelengths.

The light source for the OAS was a 100-W tungsten halogen lamp dispersed by a quarter-meter monochromator and focused onto the sample (spot size about 2 mm in diameter). The transmitted light was detected directly with a cooled Ge detector. In this configuration we reach a spectral resolution of about 1 meV . For higher resolution we used the quarter-meter monochromator with wide slits as a broadband light source, which can cover an energy range of 50 meV . The transmitted light was then detected in the PL measurement configuration.

TABLE I. Sample parameters of MQW structures with different well widths and the corresponding energy positions and binding energies of the first excitonic transition (hh_1-e_1) measured by OAS. The well width (L_w) of samples *D–G* and barrier width (L_b) were determined by TEM with an accuracy of $\pm 0.5 \text{ nm}$, of samples *A–C* estimated from growth rate measurements with a relative accuracy of better than 10%. The In content (x_{In}) was deduced from the hh_1-e_1 transition with an absolute error of $\pm 0.5\%$ to 1% (depending on the inaccuracy of the well width). The errors for the transition energy [$E(hh_1-e_1)$] and the exciton binding energy (E_{exciton}) are ± 0.2 and $\pm 0.5 \text{ meV}$, respectively. FWHM = full width at half maximum.

Sample	L_w (nm)	L_b (nm)	x_{In} (%)	Number of wells	$E(hh_1-e_1)$ (eV)	FWHM (meV)	E_{exciton} (meV)
<i>A</i>	1	20	13.5	60	1.5020	1.2	4.2
<i>B</i>	2	40	13.5	40	1.4840	1.6	7.0
<i>C</i>	3	60	13.5	20	1.4602	2.6	7.8
<i>D</i>	5	85	22	20	1.3588	6.7	9.0
<i>E</i>	7.5	85	22	20	1.3058	4.6	8.3
<i>F</i>	10.7	85	13	10	1.3907	2.8	7.0
<i>G</i>	15	80	13	10	1.3858	2.8	6.6

TABLE II. Energy position and linewidths of PL peaks from two SQW samples. Sample *H* is without Al and sample *I* is with 14% Al in the barriers, L_z =well width, $E(\text{PL})$ =energy position of the high-energy peak, FWHM=full width half maximum of the peak, LW (high)=linewidth of the high-energy peak, LW (low)=linewidth of the low-energy peak. The well widths were measured by TEM with an accuracy of ± 0.5 nm for $L_z \geq 5$ nm and estimated from the growth time relation for $L_z < 5$ nm. The error for the PL peak position is less than ± 0.2 meV. The accuracy for the determination of the high-energy linewidth is ± 0.1 meV and above 0.2–0.5 meV for the low-energy linewidth. The virtual discrepancy between FWHM and the other linewidths is due to the different peak separations and intensity ratios. Blank spaces indicate the absence of wells.

L_z (nm)	Sample <i>H</i>				Sample <i>I</i>			
	$E(\text{PL})$ (eV)	FWHM (meV)	LW (high) (meV)	LW (low) (meV)	$E(\text{PL})$ (eV)	FWHM (meV)	LW (high) (meV)	LW (low) (meV)
0.75	1.5076	0.7	0.6	1.2	1.6594	2.4	1.1	3.8
1.25	1.4994	0.9	0.8	2.2	1.6111	4.5	2.4	5.3
2.5	1.4755	2.4	1.1	2.5	1.5462	5.5	3.2	5.7
3.75	1.4518	2.8	1.5	2.9				
5	1.4331	3.4	1.5	3.1	1.4621	3.6	2.6	4.7
6.25	1.4177	3.3	1.3	2.8	1.4382	3.0	1.9	4.3
8.75					1.4094	2.6	1.9	3.7
12.5	1.3806	1.6	1.1	2.9	1.3884	3.2	1.7	3.7
25	1.3654	1.5	0.7	2.8	1.3709	3.1	1.5	3.5

With this method we can directly compare PL with OAS results and determine the Stokes shift without calibration failures.

The absorption spectrum of the interesting structure was deduced by dividing the transmission spectrum with a reference spectrum of a corresponding GaAs substrate sample. The logarithm of the inverse transmission is directly proportional to the absorption coefficient [$\alpha \sim -\ln(\text{transmission})$].

III. RESULTS AND DISCUSSIONS

A. Exciton binding energy

In Fig. 1 an absorption spectrum of a MQW sample with a 3-nm well width is shown as an example (identical

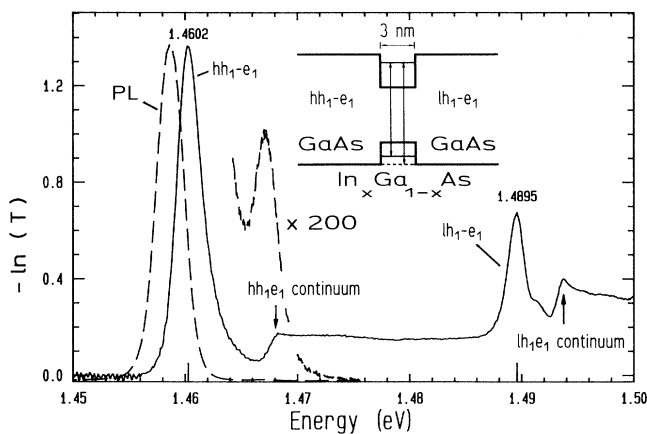


FIG. 1. Absorption spectrum (solid line) and PL spectrum (dashed line) of an $\text{In}_x\text{Ga}_{1-x}\text{As}/\text{GaAs}$ MQW sample with a 3-nm well width measured at 2 K (cf. sample *C* of Table I). The absorption coefficient α is proportional to the negative logarithm of the transmission T [$\alpha \sim -\ln(T)$]. The inset shows the optical transitions in a schematical band structure which corresponds to the labeled peaks.

to sample *C* of Table I). For this spectrum the high-resolution mode of the transmission setup was used. The dashed line shows the corresponding PL spectrum. From the distance between the PL and OAS peak we can determine a Stokes shift of 1.5 meV, which indicates a high optical quality. Because of the thin quantum well only the first-electron, heavy-hole, and light-hole states are confined (cf. inset of Fig. 1). Therefore we can only detect two transitions, which are labeled in the figure as hh_1-e_1 and lh_1-e_1 . From the energy difference between the hh_1-e_1 excitonic peak and the sharp onset of the exciton continuum we can directly deduce the exciton binding energy. We take this relatively sharp onset as the excitonic continuum rather than as the $2s$ exciton peak because this transition is damped and does not allow us to distinguish clearly whether it is a peak or the continuum. This interpretation might give rise to a scale error for the binding energy. In Table I the measured peak positions of the hh_1-e_1 peak and the corresponding exciton binding energies of seven samples with comparable In content are summarized.

The comparison of PL and OAS (cf. Fig. 1) shows a correlation between an additional weak high-energy peak of the PL spectrum and the onset of the exciton continuum in the absorption spectrum, which we can observe in the most samples. This high-energy peak has nearly the same energetic distance from the main PL peak as the corresponding value of the exciton binding energy. We therefore conclude that this peak arises from the exciton continuum. This means on the other hand that we can measure the band gap in samples with high optical quality even with a PL experiment alone.

The dependence of the exciton binding energies on the well width is illustrated in Fig. 2. The error bars are plotted according to the accuracy mentioned in Table I. For comparison the theoretical behavior of the exciton binding energy for two heavy-hole in-plane masses (m_{xy} =mass for movement parallel to the layer) is shown according to the calculations of Moore *et al.*⁸ Within the error bars we see good agreement with their experi-

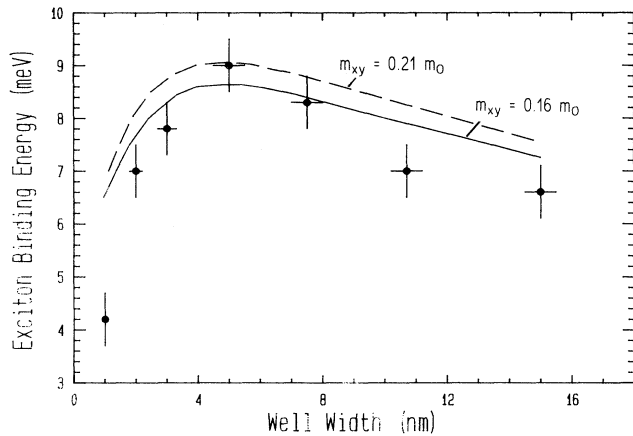


FIG. 2. Exciton binding energies of seven samples with different well widths (cf. Table I). The solid line represents calculations with an in-plane heavy-hole mass (m_{xy}) of $0.21m_0$, the dashed line of $0.16m_0$, according to Moore *et al.* (Ref. 7). Further explanations are given in the text and in Table I.

mental data between 2 and 5 nm. Our experimental data show also the expected behavior of decreasing binding energy towards thinner and thicker quantum wells. With the 1-nm MQW structure (sample *A*) we nearly reach the GaAs bulk value. The maximum at about 5 nm is well predicted too, but qualitatively there is an overestimation of the exciton binding energy especially for thicker and thinner well widths, which cannot be fitted only by varying the in-plane heavy-hole mass.

The high-energy region of the absorption spectrum in Fig. 1 shows the lh_1-e_1 transition. Because of the narrow linewidth of only 1.6 meV we can well resolve the onset of the continuum, which is related to the light-hole transition. From the distance between peak and continuum edge we can determine an exciton binding energy of 4.0 ± 0.5 meV. For the other well widths the transition was damped too strongly to measure a binding energy with useful accuracy. The large value we find gives additional evidence to a model, where the light hole is localized in the $\text{In}_x\text{Ga}_{1-x}\text{As}$ well material.¹⁰

In the high-energy shoulder of the lh_1-e_1 main peak an additional peak appears in a distance of 1.5 meV. One of the reasons can be a splitting effect because of intermixing of light- and heavy-hole states due to the large penetration depth of the light-hole wave function into the GaAs layers. Another reason, which we cannot exclude, is the possibility of a spatially indirect transition, which would possess a lower exciton binding energy than a direct transition.¹¹

B. Photoluminescence linewidth

Since the first suggestion by Weisbuch¹² it is commonly accepted that the linewidth of the emission peak is a measure of the interface quality. As a consequence the linewidth has to increase with decreasing well width, because small changes in well width lead to large changes in quantization energy in thinner wells. We show that this

is only partially true. Our experiments show that the linewidth of the excitonic transition will increase and then, after a maximum, decrease again with decreasing well width (such a behavior was already shown by Bertollet *et al.*^{5,6}) because at very small well widths the localization of the carriers is reduced and the exciton is influenced by the quality of the barrier material. So the excitonic emission shows the transition from a two-dimensional exciton to a bulklike exciton and as a consequence the influence of the interface roughness is reduced. This we will demonstrate by showing the results of $\text{In}_x\text{Ga}_{1-x}\text{As}$ quantum wells with GaAs and $\text{Ga}_y\text{Al}_{1-y}\text{As}$ barriers.

In Fig. 3 a PL spectrum of an $\text{In}_x\text{Ga}_{1-x}\text{As}/\text{GaAs}$ sample with eight quantum wells is shown. We can correlate each peak to its quantum well with its corresponding thickness (labeled in Fig. 3). At higher energies the PL intensity decreases very rapidly. The PL signal of the thinnest quantum well (0.75 nm, cf. inset of Fig. 3) was detected with a more sensitive GaAs detector at higher excitation power. On the low-energy side of the 0.75-nm well peak we can see again a band-to-band feature, but this corresponds to the 1.25-nm well. The high-energy background must be due to GaAs-related transitions.

All peaks show a fine structure, which can be fitted very accurately by only two Gaussian curves. This behavior is most pronounced for quantum wells with a thickness around 5 nm (cf. inset of Fig. 4). In both samples the low-energy peaks are approximately twice as broad as the high-energy peaks. The peak separation is also a function of the well width and varies from zero (0.75-nm well peak of sample *H*) to 1.8 meV (6.25-nm well peak). The separation is too small for complete monolayer fluctuations, which is not surprising because the exciton averages about an area of the exciton diameter at the interfaces, which cannot be strictly atomically

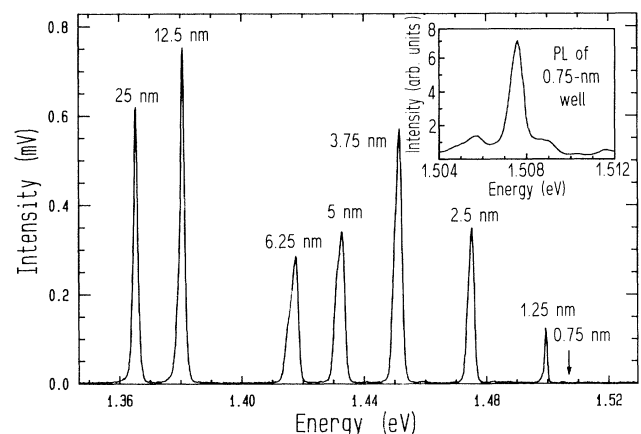


FIG. 3. PL spectrum of an $\text{In}_x\text{Ga}_{1-x}\text{As}/\text{GaAs}$ sample with a SQW sequence (cf. sample *H* in Table II) with well widths from 25 to 0.75 nm (labels at the top of each peak). The spectrum was measured at 2 K with a S1 photomultiplier at an excitation power of 1.5 W/cm^2 . The inset shows the expanded energy range of the 0.75-nm well peak, which was measured with a GaAs detector at an excitation power of 15 W/cm^2 .

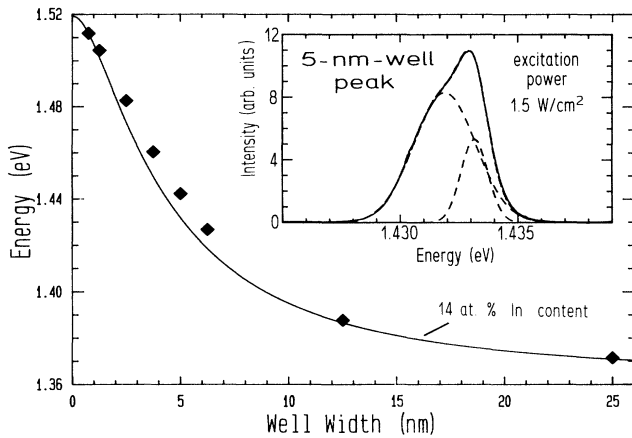


FIG. 4. PL transition energies of sample *H*, including the exciton binding energy according to Fig. 2, vs well width. The solid line was calculated with a band offset of $\Delta E_c/\Delta E_g=0.61$ and an In content of 14%. The inset shows a plot of a peak analysis with two Gaussian curves (dashed lines) of the PL peak of the 5-nm well. The cumulative curve (also dashed line) is nearly identical to the experimental curve (solid line).

flat in binary-to-ternary or even ternary-to-ternary material transitions. Therefore arbitrary values for the peak separation corresponding to thickness fluctuations up to a few monolayers are possible.¹³ The simultaneous occurrence of two peaks with systematically different linewidths must be due to exciton recombination in areas with different interface roughness spectrum. Experiments about these effects will be discussed in a forthcoming paper.¹⁴

The data of this sample (*H*) and of a sample with 14% Al in the barriers are collected in Table II. The second sample (*I*) consists of nine wells. However, the 3.75-nm well peak interferes with the intrinsic GaAs-related photoluminescence and cannot be resolved.

The energetic positions of the high-energy part of the PL peaks, which should have the smallest Stokes shifts, are visualized versus the well width in Fig. 4. For comparison with calculated transition energies, the exciton binding energies from Fig. 2 are added to the PL peak positions. The solid line is calculated according to Ref. 15 with a conduction-band offset ratio of $\Delta E_c/\Delta E_g=0.61$. At larger well widths we can determine the In content to 14%. The transition energy of the 25-nm well photoluminescence is only a few meV away from the bulk value of the strained well material. At thinner quantum wells the transition energies converge to the bulk value of the GaAs barrier material [$=1.5192$ meV at 2 K (Ref. 1)].

In Fig. 5 the high-energy linewidths of both samples are plotted versus the well width. The dependence of the linewidth on the well width is similar to the behavior of the exciton binding energy. We can also follow the transition from a situation in thick wells, where the interface roughness is less important, to a situation where the interface roughness is most important (at a 3–5-nm well width, depending on the influence of the interface), and finally to a situation at very thin wells, where the optical

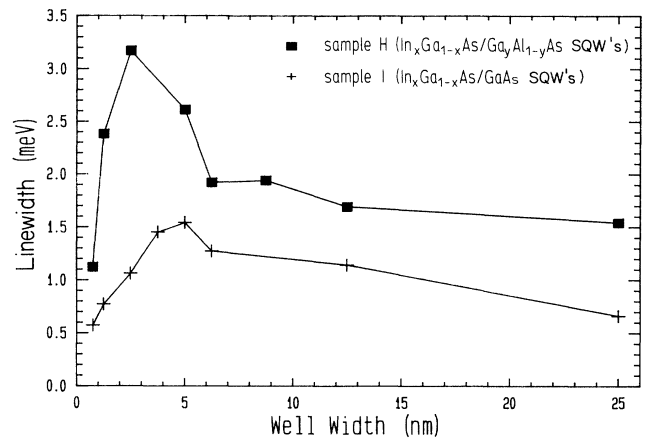


FIG. 5. Comparison of PL linewidths of two quantum-well samples with (square) and without (cross) Al in the barriers (cf. sample *H* and *I* in Table II). The high-energy part of the PL peak was always used (cf. inset of Fig. 4).

quality of the barrier material is dominant.

The influence of the barrier material is confirmed by introducing Al containing barriers. Al in the barriers reduces the material quality of the barriers, which increases the linewidth of the PL peaks of sample *I* for very thin wells. Within the 25-nm well peak (FWHM 1.5 meV) of sample *H* (binary barriers) we reach nearly the theoretical limit for dominated alloy scattering.⁴ Therefore the difference between samples *H* and *I* for a well width thicker than 3 nm must be due to interface roughness scattering. A further indication is the more pronounced line broadening at thinner quantum wells and the pushing of the maximum towards zero well width in comparison to sample *H*. But nevertheless we can observe, to our knowledge for the first time, even in ternary-to-ternary quantum-well structures a decrease of the linewidth with decreasing well width.

IV. CONCLUSIONS

We have experimentally shown on MBE-grown $\text{In}_x\text{Ga}_{1-x}\text{As}/\text{GaAs}$ MQW and $\text{In}_x\text{Ga}_{1-x}\text{As}/\text{Ga}(\text{Al})\text{As}$ SQW samples the transition from three- to two-dimensional behavior of essential excitonic properties as linewidth, energetic position of the transition, and exciton binding energy, which have a strong dependence on the well width.

With high-resolution optical-absorption measurements we could directly determine the exciton binding energy from the absorption spectrum. The spectrum of a high-quality $\text{In}_x\text{Ga}_{1-x}\text{As}/\text{GaAs}$ MQW sample with a 3-nm well width shows even a well-resolved separation of the lh_{1-e_1} exciton from the onset of the corresponding exciton continuum. The exciton binding energy for the hh_{1-e_1} exciton agrees qualitatively very well with the present theory⁸ while quantitatively there is a significant deviation for thinner and thicker wells. A high-energy PL peak was observed in all high-quality samples, which correlates with the onset of the exciton continuum and can be labeled as band-to-band transition.

All PL lines show a fine structure with a broad low energetic and a narrow high energetic peak. The dependence of the energetic position of the optical transition and the linewidth on the well width could be followed from 25-nm wells ($\text{In}_x\text{Ga}_{1-x}\text{As}$ well properties) to 0.75-nm wells (GaAs barrier properties). The comparison between samples with and without Al in the barriers gives evidence of the dominance of interface scattering in Al containing quantum-well structures. However, in an $\text{In}_x\text{Ga}_{1-x}\text{As}/\text{Ga}_y\text{Al}_{1-y}\text{As}$ SQW sample with 14% Al in

the barriers we have also observed a strong decrease of the linewidth towards zero well width.

ACKNOWLEDGMENTS

We wish to thank D. Bernklau for sample preparation, A. Miklis for assistance in optical measurements, and C. Fruth and V. Huber for thickness determination by TEM. We gratefully acknowledge general support by H. Schlötterer.

*Present address: IBM Research Laboratories, Säumerstrasse 4, 8803 Rüschlikon, Switzerland.

¹*Landolt-Börnstein, Numerical Data and Functional Relationships in Science and Technology, New Series, III/17a*, edited by O. Madelung (Springer, Berlin, 1982).

²U. Heim and P. Hiesinger, *Phys. Status Solidi B* **66**, 461 (1974).

³G. Bastard, E. E. Mendez, L. L. Chang, and L. Esaki, *Phys. Rev. B* **26**, 1974 (1982).

⁴P. K. Basu, *Appl. Phys. Lett.* **56** (12), 1110 (1990).

⁵D. C. Bertolet, J.-K. Hsu, S. H. Jones, and K. M. Lau, *Appl. Phys. Lett.* **52** (4), 293 (1988).

⁶D. C. Bertolet, J.-K. Hsu, K. M. Lau, E. S. Koteles, and D. Owens, *J. Appl. Phys.* **64**, 6562 (1988).

⁷J. W. Matthews and A. E. Blakeslee, *J. Cryst. Growth* **27**, 118 (1974).

⁸K. J. Moore, G. Duggan, K. Woodbridge, and C. Roberts, *Phys. Rev. B* **41**, 1090 (1990).

⁹A. J. SpringThorpe, S. J. Ingre, B. Emmerstorfer, P. Mandeville, and W. T. Moore, *Appl. Phys. Lett.* **50**, 77 (1987).

¹⁰J.-P. Reithmaier, R. Höger, H. Riechert, P. Hiergeist, and G. Abstreiter, *Appl. Phys. Lett.* **57**, 957 (1990).

¹¹G. Bastard, *Wave Mechanics Applied to Semiconductor Heterostructures, Nonographies der Physique* (Les Éditions de Physique, Les Ulis, 1988), p. 135.

¹²C. Weisbuch, R. Dingle, A. C. Gossard, and W. Wiegmann, *Solid State Commun.* **38**, 709 (1981).

¹³C. A. Warwick, W. Y. Jan, A. Ourmazd, and T. D. Harris, *Appl. Phys. Lett.* **56**, 2666 (1990).

¹⁴J.-P. Reithmaier, R. Höger, and H. Riechert (unpublished).

¹⁵J.-P. Reithmaier, R. Höger, H. Riechert, A. Heberle, G. Abstreiter, and G. Weimann, *Appl. Phys. Lett.* **56**, 536 (1990).